Axial segregation of granular media rotated in a drum mixer: Pattern evolution

K. M. Hill,[1] A. Caprihan,[2] and J. Kakalios[1]
[1]*School of Physics and Astronomy, The University of Minnesota, Minneapolis, Minnesota 55255*
[2]*The Lovelace Respiratory Research Institute, 2425 Ridgecrest Drive Southeast, Albuquerque, New Mexico 87108*
(Received 12 May 1997)

In the traditional axial segregation effect, a homogeneous mixture of different types of granular material rotated in a drum mixer segregates into surface bands of relatively pure single concentrations along the axis of rotation. This effect primarily has been studied with respect to the initial segregation. However, the initial pattern is not stable, but evolves in time with continued rotation through metastable states of fewer and fewer bands. We describe two experimental studies of this evolution that provide a more complete picture of the dynamics involved in the pattern progression. The use of a charge coupled device camera in conjunction with digital analysis techniques provides a quantitative measure of the state of the surface as a function of time, while magnetic resonance imaging techniques provide a noninvasive method for studying the segregation beneath the surface. These methods indicate that the underlying mechanisms for the pattern evolution may originate in the bulk of the material, beneath the avalanching surface. [S1063-651X(97)04910-6]

PACS number(s): 81.05.Rm, 46.10.+z, 47.27.Te, 64.75.+g

I. INTRODUCTION

Granular media such as sand and powders exhibit a range of fascinating behaviors that can lead to practical problems when processing granular materials in, for example, pharmaceutical and agricultural industries. These include properties such as dilation and arching that have been studied for some time [1] and others such as oscillons in vibrated granular materials, which only recently have been discovered [2]. Some of the properties that lead to complications in the processing of granular materials include the nonlinear pressures exerted by grains on the side walls of silos or other storage containers and the tendency of granular materials to separate. (See, for example, Refs. [3,4].) Mixtures of granular materials such as powders and sand tend to segregate by particle property, which is a significant industrial problem as well as an interesting phenomenon in nonlinear pattern formation.

Granular materials often segregate even in situations where one is trying to mix the different components. In particular, some granular mixtures will segregate when they are rotated in a horizontal cylinder in a manner similar to the motion of a drum mixer, as indicated by the arrows indicating motion around the dotted line in Fig. 1. When certain binary mixtures of different-sized granular materials are rotated in this way, the components in the mixture will first radially segregate, with the smaller component becoming more highly concentrated near the center of the bulk. In a systematic study of segregation in a rotating drum, Donald and Roseman described the cause of radial segregation *and* mixing in terms of the movement of particles from one circulation path (closer or farther from the center of rotation) to another. Radial segregation, they claimed, was due to the higher likelihood of the smallest particles in a faster flowing circulation layer to become trapped within the gaps of the more slowly flowing layer beneath it and thus to move into that circulation path closer to the center of rotation [5]. On the other hand, Clement, Rajchenbach, and Duran cited evidence that the phenomenon was based on a stochastic bistability where there were two competing attractors for the particles. One attractor, near the outer edge, kept larger particles near the edge, away from the center of rotation. The other attractor near the axis of rotation drew smaller particles towards the center [6]. A third explanation was based on the

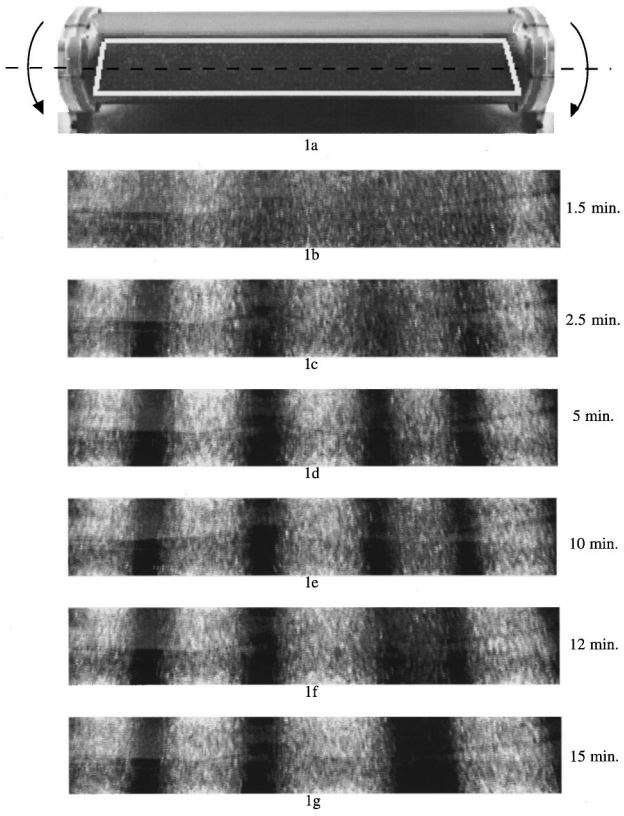

FIG. 1. Surface images of the granular mixture taken while it was rotated. The images in (b)–(g) were taken while the cylinder continuously rotated. The location of these images is indicated by the white box in (a). (b) was taken after 1.5 min of rotation, (c) after 2.5 min of rotation, (d) after 5 min of rotation, (e) after 10 min of rotation, (f) after 12 min of rotation, and (g) after 15 min of rotation.

theory of Mehta, Edwards, and Oakshott on the statistics of granular materials [7,8]. Hill and Kakalios claimed the radial segregation to be due to variation in compactivity in the flowing layer extending from the axis of rotation to the freely flowing top surface [9]. The reader is referred to a number of reports on experiments [6,10] and simulations [11,12] that examine the radial segregation in more detail. While the radial segregation effect is not extensively investigated in this report, which is primarily concerned with axial segregation, radial segregation plays an important role in the evolution of the axially segregated bands as described below.

After radial segregation occurs, as the cylinder continues to rotate, some mixtures segregate further into what appears from the surface to be bands of relatively pure single concentration along the rotational axis, as illustrated in the photographs in Figs. 1(a)–1(d), termed axial segregation [5,9,13–18]. Some mixtures of granular materials also exhibit a reversible axial segregation, wherein the bands disappear when the rotation speed is decreased [effectively following the reverse process, in the pictures from 1(d) to 1(a)] [9]. As shown in Figs. 1(e)–1(g), the initial segregation pattern resulting from rotation at higher speeds is only temporary. When a mixture that has segregated into bands continues to rotate at the same speed, the original pattern of bands usually evolves into one with a smaller number of bands that are wider than those in the original configuration [9,16,17].

An initial report of axial segregation was by Oyama in 1939 [13]. A theory was developed to explain axial segregation in terms of surface flow and an effective diffusion equation [15,16], which was successfully modified and adapted to explain the reversible effect [9]. In 1993, Savage reported observing pattern evolution in an axially segregating system [16]. Later, other groups [9,17] also reported observing the merging of bands with continued revolution. However, none of these authors had an explanation for the pattern development nor the dependence of system wavelength on specific parameters beyond the natural coarsening that might occur with time in a system driven by an effective diffusion equation. Savage developed a cellular autonoma model patterned after the diffusion equation theory that successfully imitated the development of a metastable pattern of bands, as well as the merging of bands, often triggered by a random fluctuation [16]. He acknowledged, however, that the cellular autonoma model and the explanation for axial segregation involving an effective diffusion equation oversimplify the details involved. The actual flow is more complex as it involves radial as well as axial movement of particles.

When two bands merge in a real system, they do not, in general, simply move toward each other until they meet. Rather, in the case of the merging of two small bead bands as shown in Fig. 1, for example, it appears from the surface that the region between the small bead bands becomes increasingly more concentrated with small beads, while the small bead concentration within the bands themselves appear to decrease slightly, until the concentration of all three regions is roughly uniform. Finally, a new single band of small beads ''sharpens.'' That is, the band itself narrows while the region within it becomes more highly concentrated with small beads. The pattern is then stable again with only minor axial movement of the bands until the next relatively sudden merging event occurs. The time dependence of the pattern development as well as the details of subsurface interactions may have strong implications for the understanding of axial segregation. However, the pattern development remains poorly understood, in part due to the difficulty of obtaining quantitative measurements of the state of the system as a function of time.

In this paper we describe two imaging techniques used to experimentally study the pattern development of the axially segregated bands in rotated granular materials. Digital images were taken with a charge coupled device (CCD) camera while the system was rotated to provide quantitative information of the state of the surface segregation and the relevant time and length scales of the pattern development. These studies are complemented by magnetic resonance imaging (MRI), which provides a method for noninvasively examining concentrations and other details beneath the surface of granular materials [19–24]. The description of the digital analysis of the surface segregation will be presented in Sec. II as well as results for a system of a binary mixture of spherical particles. Statistical analysis supports surface observations that some local remixing is associated with band merging events. Therefore, interactions beneath the surface are at least in part responsible for the band evolution. Furthermore, systematic pattern development studies done with one system indicates that the rate and form of the pattern development vary with different rotation speeds. This would indicate that subsurface dynamics vary with changing rotation speed. In Sec. III the MRI methods used for obtaining information about the concentration variations beneath the surface will be presented as well as results that provide additional evidence for the subsurface interactions that lead to band merging. In Sec. IV we will conclude with plans for future studies including dynamic MRI measurements to examine the rotation speed dependence of subsurface dynamics.

II. DIGITAL SURFACE ANALYSIS

The experimental apparatus for the surface segregation studies is similar to that in Ref. [9]. The drum mixer used was a 61-cm-(2-ft-) long Plexiglas cylinder with a 6.4-mm-thick ($\frac{1}{4}$-in.) wall, 12.5 cm (5 in.) in diameter, rotated about its axis with a $\frac{1}{17}$-hp motor (providing rotational speeds up to approximately 100 rpm). For the images in Fig. 1 the cylinder was one-third filled with a 50/50 mixture by volume of 0.75-mm-diam (dark) and 3.0-mm-diam (clear, appearing light) glass spheres. The specific gravity of both large and small glass beads is 2.55. While the mixture was rotated in the cylinder, digital images were taken at regular time intervals with a Cohu 4915 CCD camera and Scion LG-3 frame grabber operated with the public domain NIH image software on a Power Macintosh. Figure 1 shows such images taken through the cylinder wall. The box in Fig. 1(a) indicates the region from which the data in the remainder of Fig. 1 were taken. The regions near the end plates were not included in this analysis as, unlike the majority of the axial bands farther from the end plates, the development of the bands near the ends of the cylinder appear to depend largely on end-plate–bead interactions and evolves differently from the rest of the pattern [9].

For the system illustrated in Fig. 1, after 1.5 min of rota-

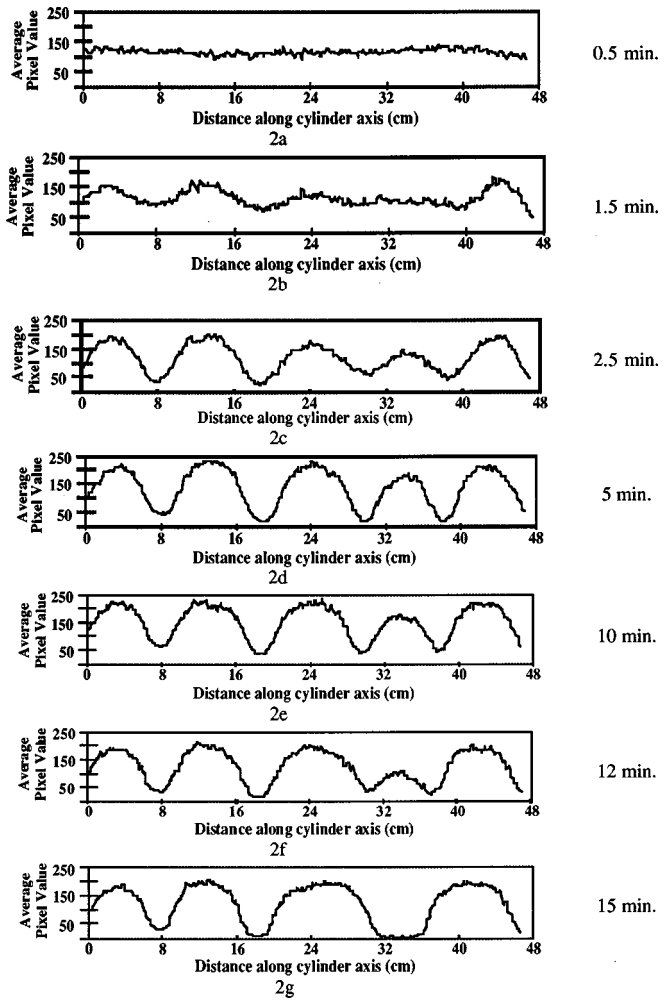

FIG. 2. Results from digital image analysis for the mixture shown in Fig. 1. (a)–(f) show the average pixel intensity (in arbitrary units) as a function of distance along the cylinder axis for the images shown in Figs. 1(a)–1(f).

tion at approximately 15 rpm [Fig. 1(b)] a hint of axial segregation is visible. After 2.5 min of further rotation at 15 rpm, the beginning of axial segregation is more clearly observed [Fig. 1(c)]. After 5 min of rotation, clear segregation of the large and small beads into sharp bands is achieved [Fig. 1(d)]. The system shown in Fig. 1 appeared stable for the next 5 min of rotation; the image taken at 10 min [Fig. 1(e)] is similar to the one taken after 5 min of rotation. However, after an additional 2 min. [see Fig. 1(f)], it was clear that the pattern was changing. As mentioned above, the two bands did not appear to simply move toward each other until they merged. Instead, the concentration of small dark beads increased beneath the surface within the large bead band, which was soon to be lost in the merging event. This small bead concentration continued to increase until the three regions became one wider band of small beads. The system reached the new metastable state after approximately 3 min more of rotation [Fig. 1(g)].

Figures 2(a)–2(g) show the average intensity as a function of position along the cylinder axis for the images in Figs. 1(a)–1(g), respectively. Since the pixel value at each point corresponds to the concentration of the mixture, the development of axial segregation can be evaluated from studying changes in these average pixel values as a function of time. The 0.75-mm beads are dark and the 3.0-mm beads are clear. Thus a high intensity in the graphs of Figs. 2(a)–2(g) corresponds to high concentration of large beads near the surface, a low intensity indicates a high concentration of small beads, and an intermediate intensity reflects a mixture of the two. Figure 2(a) shows the mixture ratio as a function of axial distance for the area outlined in Fig. 1(a) after only 30 s of rotation. Figures 2(b)–2(d) correspond to the images in Figs. 1(b)–1(d) when the mixture had been rotated for 1.5, 2.5, and 5 min, respectively, while the bands were first forming. Figures 2(e)–2(g) correspond to the images in Figs. 1(e)–1(g) and show some of the intensity data during the merging event. As suggested by surface observation, these traces indicate that the band merging event does not involve two bands moving together. While the third and fourth valleys, representing the third and fourth small bead bands, remain centered around 30 and 38 cm from the end, respectively, the peak between them representing the concentration within the large bead band drops, especially apparent in Fig. 2(f). The final single band of small beads in that region is represented by the wide trough in Fig. 2(g).

These data can be converted into a comprehensive image, with the values for the average intensity for each image in Fig. 2 reconverted to a string of pixel values and pasted together to form a time line for the pixel values, as shown in Fig. 3(a). Since the images were taken at a rate of two per minute, there is a vertical string of pixels every 30 s. (The image may be easier to interpret if turned 90°). Figure 3(b) is a graph of the mean value (dotted line) and the standard deviation of the mean (solid line) for similar traces as shown in Fig. 2 also taken from images during the entire experiment. The approximate locations on the graph for the images and graphs in Figs. 1(a)–1(g) and 2(a)–2(g), respectively, are indicated and one can also follow the development of the segregation in the image in Fig. 3(a).

The mean value (dashed line) is roughly constant in time, indicating no loss of beads of either type and no loss of information beneath the surface. On the other hand, the standard deviation is closely related to the state of segregation. When the mixture is fairly uniform in distribution, as indicated by *a* in Fig. 3(b), the pixel value at every point in the surface is fairly close to the mean value and the standard deviation of the mean is low. If the bands are sharply defined, the pixel values in images taken of the surface should be far from the mean value. Thus the sharp rise (through *b* and *c*) in the standard deviation in the graph corresponds to the initial formation of the bands, until the bands finally sharpen after approximately 5 min of rotation, indicated by *d*. While casual surface observation suggest that nothing is changing while the cylinder is rotated for the next 5 min, the dip in the standard deviation as the bands are merging suggests otherwise. The continuous slope indicates that the band development is a continuous process. Between *e* and *f* the local minimum occurs, when surface observations indicate subsurface interactions and local remixing occurs during a band merging event. When the band number is finally reduced, there are fewer band-band interfaces and thus fewer regions closer to the mean value of the traces, which is presumably why the next semistable pattern (indicated by *g* in Fig. 4) has a higher standard deviation than the previous one.

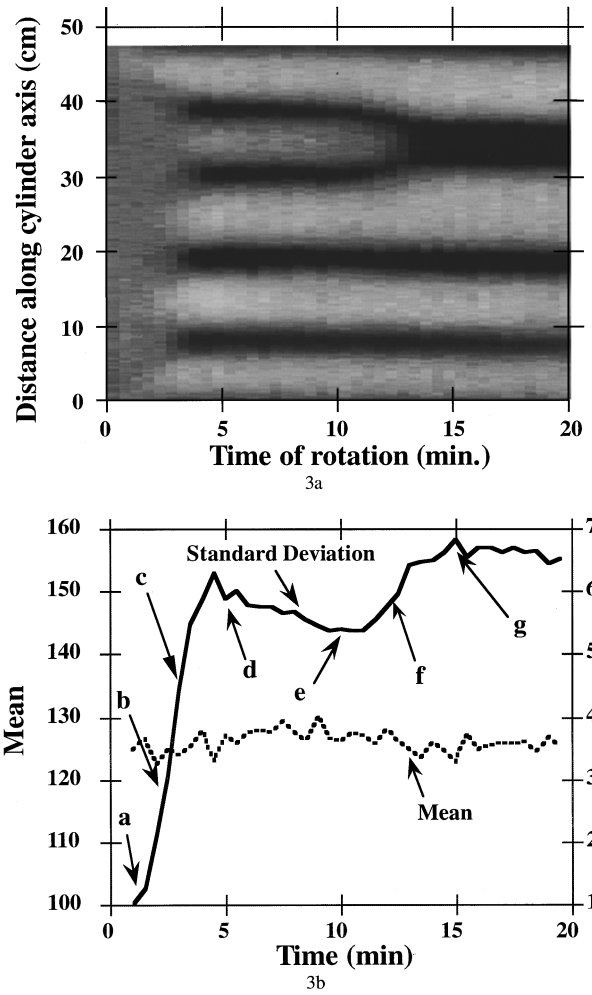

FIG. 3. Compilations of the data of Figs. 1 and 2 from images taken during the entire experiment (total rotation time of 20 min), for measurements taken every 30 s. (a) shows the pattern development graphically by reconverting the average pixel values from the traces (as in Fig. 2) into gray-scale images and thus representing each time step by a vertical string of pixels. (b) is a graph of the mean value and the standard deviation of the mean for these traces. The approximate locations on the graph for images and graphs of Figs. 1(a)–1(f) and 2(a)–2(f), respectively, are indicated.

The same analysis was done for a 50/50 mixture of 0.75-mm (dark) spheres and 1.5-mm (light) spheres, also of specific gravity 2.55. The pattern development was followed for speeds ranging from just under 4 rpm to almost 100 rpm. This mixture exhibited qualitatively different segregation and evolution behaviors at the different speeds, as demonstrated in Fig. 4. Figure 4(a) is the comprehensive image of the pattern development [as in Fig. 3(a)] for the images taken of the pattern evolution when the system was rotated at 4.9 rpm and Fig. 4(b) is the graph of the mean and standard deviation [as in Fig. 3(b)]. Figures 4(c) and 4(d) contain the corresponding information for one run performed at 11.4 rpm and Figs. 4(e) and 4(f) contain the data from a run taken with the cylinder rotating at the highest speed measured: 97.6 rpm. Clearly, the initial segregation occurs more quickly at higher speeds. The initial time for segregation in some cases is related to the speed of rotation via a power law and is planned to be discussed elsewhere [25]. This increased rate of segregation at higher rotation speeds may be caused by a number of factors, for example, an increase in the velocity and thickness of the flowing layer when the speed of rotation is increased [20,26].

Once the banding pattern has developed initially, the evolution of the bands can differ tremendously depending on the speed of rotation. The evolution follows one of three qualitatively different patterns depending on whether it is rotating at slow, intermediate, or high speeds. First, at slower speeds, the pattern moves through many intermediate metastable states of fewer and fewer bands. The duration of each intermediate metastable state is much shorter than the time it takes for the pattern to move from one metastable state to the next. The pattern development takes this form at speeds near the transition speed (below which the mixture does not segregate), just above 3.5 rpm, and continues for speeds up to approximately 5.5 rpm. The system in Figs. 1–3, for which the bead sizes differed from the system in Fig. 4, is operating within this first regime. This first form of the pattern development is in contrast to the pattern development observed at intermediate speeds where the pattern appears to reach a very stable state early in the rotation. Figure 4(d) shows an example of the typical result of statistical analysis of the images for these runs. The standard deviation of the mean plateaus early in the experiment for a time significantly longer than the time it takes for the system to segregate and the system remains stable for some time. The evolution of the system of 0.75 and 1.5 mm beads is similar to this for speeds between 6 rpm up to about 40 rpm.

At very high speeds, the pattern development changes qualitatively once again as shown in Figs. 4(e) and 4(f). Admittedly, it is in part similar to the pattern development at low rotation speeds in that the pattern development occurs very symmetrically, as seen in Figs. 4(a) and 4(b). In addition, the metastable states at the very low and very high speeds last for a relatively short time compared to the initial time for segregation. However, the band pattern does not evolve in the same manner as occurs at lower speeds, with bands merging, two at a time. Instead, it seems driven by the expansion of the outer two bands of small beads in towards the center while the central band of large beads is maintained. Of course, at such high rotation speeds the top avalanching surface displays strong curvature (see, for example, Refs. [27,28]) and thus it is not surprising that the segregation dynamics are changed. From the darker appearance of the image it is clear that a higher percentage of small beads are being carried up to the surface from the radial mode. This can be seen clearly in the different mean values for the different runs. (Note the difference in the scale for the different speeds.) At 4.8 and 11 rpm, the mean is approximately the same. At $\sim$100 rpm, the mean is much lower, showing more small (dark) beads being continually carried to the surface. However, the shape of the surface remains relatively flat between 4.8 and 11 rpm. Since the pattern development changes qualitatively even at these lower rotation speeds, it is likely that the form the pattern development follows is not solely driven by surface effects. If indeed the dynamics beneath the surface drive the development of the band pattern, these data show that these dynamics must vary qualitatively with speed of rotation even at the lower speeds.

The analysis of the surface images provides important in-

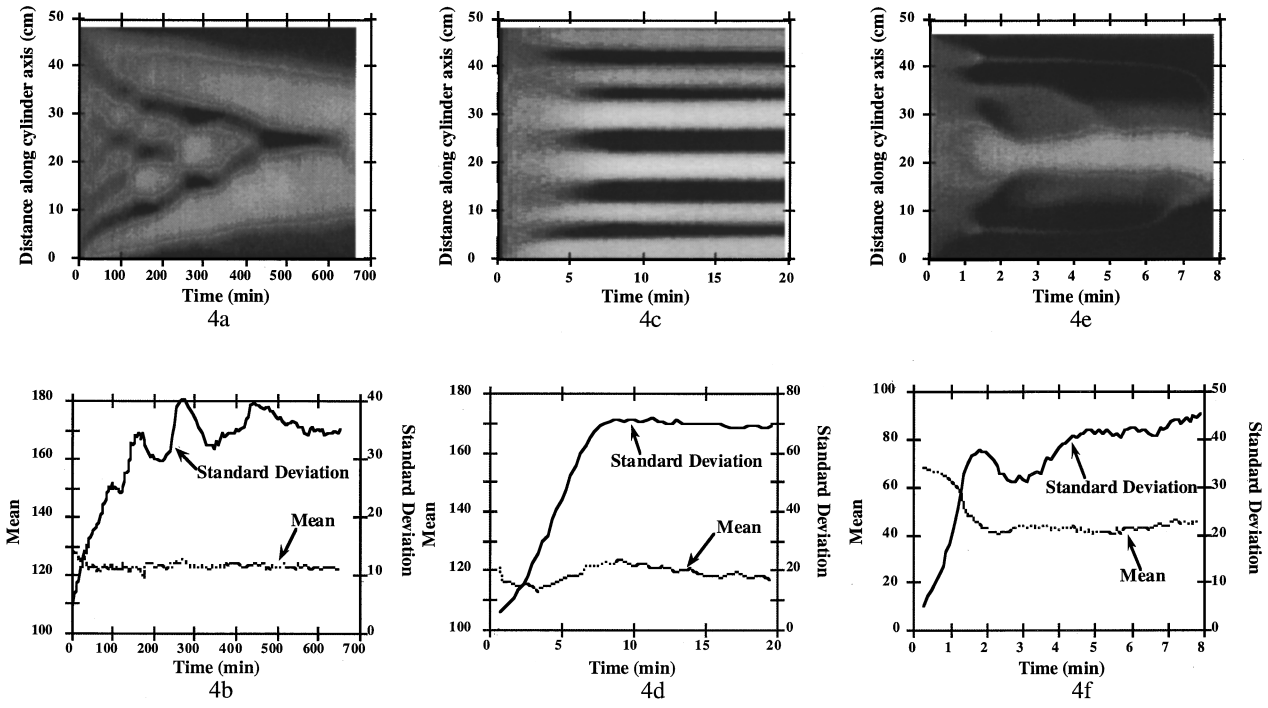

FIG. 4. Compilation images and statistical analysis (mean and standard deviation plotted against rotation time) for the pattern development of a system rotated at different speeds. (a) and (b) are plots for the system rotated at low speeds (around 4 rpm, near the transition speed below which the system will not segregate), (c) and (d) are for the system rotated at intermediate speeds (around 11 rpm), and (e) and (f) are for the system rotated at very high speeds (around 100 rpm).

formation concerning the development of the banding pattern of axially segregated systems. The results support some of the surface observations about the band merging events. In particular, the band merging events do not simply involve two bands moving together, but instead all of the bands involved become less distinct until the final band sharpens. In addition, the band merging events are not as sudden as they appear from casual surface observation, but seem to involve a more continuous process. Finally, systematic studies of band evolution in one mixture rotated at different rotation speeds find that the subsurface involvement varies at different speeds. To understand more of the details involved in the segregation, data are needed regarding the concentration changes beneath the surface.

III. MAGNETIC RESONANCE IMAGING EXPERIMENTS

In order to investigate the local remixing during band merging events magnetic resonance imaging was used. MRI allows for noninvasive observation of the evolution of the pattern within the bulk as it progresses from one stage to the next. Nakagawa and co-workers demonstrated that liquid-state MRI techniques may be used to image arbitrary planes within the bulk of granular media for material containing a fluid [20]. They have used these techniques to investigate the dynamics of granular flow in a partially filled rotating drum as well as the migration of the radially segregated core of a mixture with continued rotation [21].

In a recent report [19] we described the use of MRI to obtain a full three-dimensional picture of axial segregation by imaging planes both perpendicular and parallel to the cylinder axis at successive stages of the development of the bands. The experimental setup employed for the band development studies is similar to that in Ref. [19]. A mixture of one MRI-sensitive component and one that is not MRI active is used, so that a concentration image will directly show the distribution of the MRI active species. The MRI-sensitive beads are 1-mm-diam spherical pharmaceutical pills, while the MRI inert beads are 3-mm plastic spheres. The spheres were rotated in an acrylic cylinder, 24 cm long and 7.5 cm in diameter. Fluid-filled spheres were taped along the outside of the cylinder at 5-cm intervals to provide reference points in the images. A NMR imager-spectrometer (Nalorac Cryogenics Corp.) was used at The Lovelace Institute with a 1.9-T Oxford superconducting magnet with a bore diameter of 31 cm. The magnet bore is horizontal, so the cylinder may be placed into the magnet without disturbing its contents. Digital image analysis was performed on a Power Macintosh 7100/80 computer using the public domain NIH image program. The partially filled cylinder was first rotated outside the magnet, where the state of the surface segregation was noted. Rotation was then stopped and the cylinder was placed within the bore of the magnet where the material was imaged using standard stationary NMR imaging techniques. This procedure was repeated for extended rotation periods. In this way, the evolution of the radial and axial segregation was serially monitored. The MRI experiment images a 5-mm-thick slice either perpendicular to the axis at any point along the length of the cylinder as illustrated in Fig. 5(a) or parallel to and containing the axis of the cylinder as illustrated in Fig. 5(c). The smaller MRI sensitive spheres appear as bright regions in the images and dark regions correspond to high concentrations of the larger MRI inert spheres.

After the mixture had been rotated for approximately 5.5

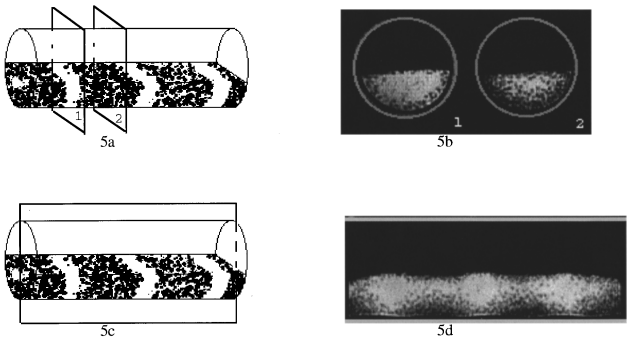

FIG. 5. MRI data for a mixture of pharmaceutical spheres (1 mm) and plastic spheres (3 mm) rotated in a 24-cm-long cylinder for 5.5 min at 30 rpm. From outside the cylinder, the mixture appears to have segregated radially and axially. (a) illustrates the state of the system as viewed from outside after rotation and the approximate locations of the planes from where the images shown in (b) were taken: within the small sphere band (1) and within the large sphere band (2). (c) indicates the location of the image taken parallel to the axis shown in (d). The brighter regions represent higher concentrations of small spheres.

min at 30 rpm in a 7.5-cm-diam 24-cm-long cylinder, the mixture appeared both radially and axially segregated on the outside as indicated in the sketch in Fig. 5(a). Images taken beneath the surface at this point indicate an interdependence between radial and axial segregation. Figure 5(a) illustrates the state of the mixture as observed from the outside, as well as the approximate location of the images taken perpendicular to the cylinder axis shown in Fig. 5(b). The images in Fig. 5(b) serve two purposes. They indicate that the high concentration of small spheres near the center of the rotational axis, the radial segregation, exists both within the bands of the smaller spheres and within the bands of the larger spheres. These images also ensure that the pattern is roughly cylindrically symmetric around the axis of rotation at any given location and thus the images containing the cylinder axis [as in Fig. 5(d)] are sufficient for a first-order representation of the state of the mixture below the surface. Figure 5(c) shows the location of the image taken down the length of the cylinder axis shown in Fig. 5(d). In Fig. 5(d) it is verified that the ''radial mode'' of small beads runs down the entire length of the cylinder, widening to the surface in the regions where axial bands of small spheres are seen from above.

Figure 6 illustrates the pattern development of this system. Figures 6(a), 6(c), and 6(e) are the subsurface images taken using MRI as two of the bands merged. These images are all vertical and parallel to the cylinder axis in the position indicated in Fig. 5(c). Figures 6(b), 6(d), and 6(f) are sketches illustrating the state of the surface extrapolated from MRI data taken near the surface. Figure 6(a) is the subsurface image taken after approximately 15 min of rotation after the mixture had radially segregated and axially segregated into three bands of small beads and four bands of large beads [as shown in Fig. 6(b)]. After approximately 8 min of further rotation, the bands had begun to merge, mostly beneath the surface as illustrated in Figs. 6(c) and 6(d). The radial mode of small beads increased significantly in the region between the small beads that were merging and that region became more highly concentrated with small beads. The bands as seen on the surface had not moved much closer together.

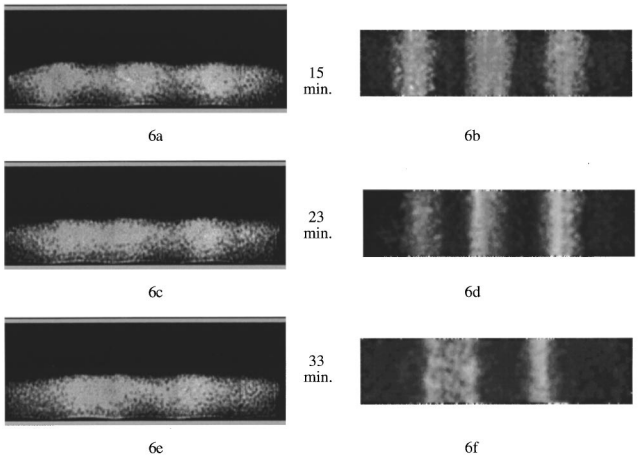

FIG. 6. (a), (c), and (e) Subsurface MRI data and (b), (d), and (f) corresponding surface illustrations for a mixture of pharmaceutical spheres (1 mm) and plastic spheres (3 mm) rotated for an extended period of time in a 24-cm cylinder at 30 rpm. The images were taken while a band merging event was occurring. (a) and (b) correspond to the state of the mixture after approximately 15 min of rotation, (c) and (d) correspond to the system after 23 min of rotation, and (e) and (f) correspond to the state of the system after 33 min of rotation. Again, brighter regions represent higher concentrations of 1-mm spheres.

Finally, after an additional 10 min of rotation the bands had completely merged, as illustrated by Figs. 6(e) and 6(f).

This qualitative description is supported graphically by the results in Figs. 7 and 8. Figures 7(a)–7(d) are the intensities of the MRI image near the surface. (These are somewhat noisier than the surface data taken with the CCD camera due to the lack of data from the entire surface for averaging.) Figures 8(a)–8(d) are the average concentrations along the axis for the MRI images. In these graphs, since the smaller 1-mm spheres are MRI sensitive, a high intensity indicates a high concentration of small beads and a low intensity indicates a high concentration of large beads. Figures 7(a) and 8(a) are data from the image in Fig. 5(d), taken after approximately 5 min of rotation at 30 rpm. Figures 7(b) and 8(b) are data from the image in Fig. 6(a), taken after approximately 15 min of rotation when surface observations indicated little (if any) change from the initial state of segregation of three bands of small beads and four bands of large beads. Figures 7(c) and 8(c) are data from the image in Fig. 6(c), while the bands were merging, and Figs. 7(d) and 8(d) are data from the image in Fig. 6(e).

One marked difference between these sets of graphs is that the graphs in Fig. 7 indicate that the bands are distinct from each other at the surface: between each pair of small bead bands the intensity is close to zero, indicating almost no small bead bands on the surface in the large bead bands (though, from the low intensity in the small bead bands compared to the average images, it is clear a number of large beads remain on the surface of the small bead bands). However, in the graphs of the average concentration, the bands do not appear as distinct. The intensity is relatively high between the small bead bands due to the radial mode. Thus the band merging events do not seem as dramatic beneath the surface, but instead appear to be a minor rearrangement of the relative concentrations, moving the system from a state

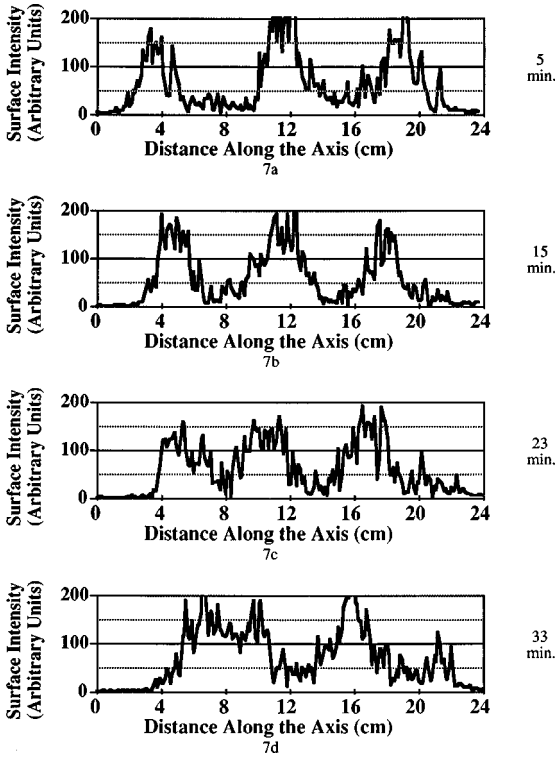

FIG. 7. MRI intensity along the top surface of the system from images taken parallel to the axis of the cylinder during the merging event. (a) is the data from the image in Fig. 5(d), (b) is the data from the image in Fig. 6(a), (c) is the data from the image in Fig. 6(c), and (d) is the data from the image in Fig. 6(e).

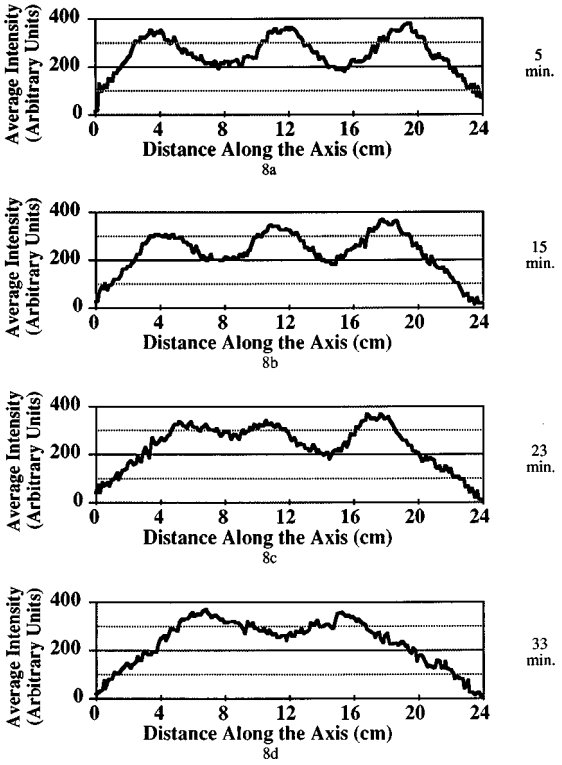

FIG. 8. Average intensity as a function of position along the axis, from the identical images used for the surface intensities in Fig. 7. (a)–(d) corresponds to the surface data in Figs. 7(a)–7(d), respectively.

of smaller pockets of each component to fewer and fewer pockets with a gradual concentration gradient from one band to the next.

IV. SUMMARY

The evolution of the axial banding pattern in a system of granular material rotated in a drum has been studied. An analysis of digital images taken of the surface segregation in conjunction with subsurface measurements using MRI techniques provides important information about the details of the evolution of the surface pattern. The data from the surface segregation show that as a band merging event occurs there is some local mixing, indicating that there are interactions beneath the surface that are driving the pattern evolution. Systematic studies of the changes in the pattern development at different rotation speeds suggest that these subsurface interactions must vary with rotation speeds. MRI data support the conjecture of subsurface dynamics driving the pattern evolution as these images reveal a relationship between the radial and axial segregation and movement in the radial mode when the axial bands are merging. Future MRI studies will involve velocity measurements within and beneath the surface to determine the mechanisms responsible for the change in dynamics with rotation speed.

ACKNOWLEDGMENTS

This research was supported in part by the Minnesota Graduate School Grant-in-Aid program, Grant No. NSF-CTS-9501437; the U.S. Department of Energy; Pittsburgh Energy Technology Center via Grant No. De-FG22-94PC94248; and the U.S. Department of Energy, Office of Basic Energy Sciences via Grant No. DE-FG03-93ER14316. We gratefully acknowledge the help and hospitality of Steve Altobelli, Eiichi Fukushima, Masami Nakagawa, Allen Waggoner, and the Lovelace Institute, where the MRI data were taken.

[1] See, for example, H. M. Jaeger and S. R. Nagel, Science **255**, 1523 (1992), and references therein.

[2] P. B. Umbanhowar, F. Melo, and H. L. Swinney, Nature (London) **382**, 793 (1996).

[3] M. H. Cooke, D. J. Stephens, and J. Bridgwater, Powder Technol. **15**, 1 (1976).

[4] L. T. Fan, Y.-M. Chen, and F. S. Lai, Powder Technol. **61**, 255 (1990).

[5] M. B. Donald and B. Roseman, Br. Chem. Eng. **7**, 749 (1962); **7**, 823 (1962).

[6] E. Clement, J. Rajchenbach, and J. Duran, Europhys. Lett. **30**, 7 (1995).

[7] S. F. Edwards and R. B. S. Oakshott, Physica A **157**, 1080 (1989).
[8] Anita Mehta and S. F. Edwards, Physica A **157**, 1091 (1989).
[9] K. M. Hill and J. Kakalios, Phys. Rev. E **49**, R3610 (1994); **52**, 4393 (1995).
[10] F. Cantelaube and D. Bideau, Europhys. Lett. **30**, 133 (1995).
[11] Ristow, Europhys. Lett. **28**, 97 (1994).
[12] Ristow (unpublished).
[13] Y. Oyama, Bull. Inst. Phys. Chem. Res. (Tokyo) Rep. **5**, 600 (1939); Y. Oyama and K. Ayaki, Kagaku Kikai **20**, 6 (1956).
[14] J. Bridgwater, N. W. Sharpe, and D. C. Stocker, Trans. Inst. Chem. Eng. **47**, T114 (1969).
[15] S. Das Gupta, D. V. Khakhar, and S. K. Bhatia, Chem. Eng. Sci. **46**, 1513 (1991).
[16] Stuart B. Savage, in *Disorder and Granular Media*, edited by D. Bideau and A. Hansen (North-Holland, Amsterdam, 1993), p. 255.
[17] M. Nakagawa, Chem. Eng. Sci. **49**, 2540 (1994).
[18] S. Fauve, C. Laroche, and S. Douady, in *Physics of Granular Media*, edited by Daniel Bideau and John Dodds (Nova Science, Commack, NY, 1991), p. 277.
[19] K. M. Hill, A. Caprihan, and J. Kakalios, Phys. Rev. Lett. **78**, 50 (1997).
[20] M. Nakagawa *et al.*, Exp. Fluids **16**, 54 (1993); S. A. Altobelli, A. Caprihan, E. Fukushima, M. Nakagawa, and R. C. Givler (unpublished).
[21] S. A. Altobelli *et al.* (unpublished); M. Nakagawa, S. A. Altobelli, A. Caprihan, and E. Fukushima (unpublished).
[22] E. E. Ehrichs, H. M. Jaeger, G. S. Karczmar, J. B. Knight, V. Y. Kuperman, and S. R. Nagel, Science **267**, 1632 (1995).
[23] G. Metcalfe and M. Shattuck (unpublished).
[24] K. M. Hill, A. Caprihan, and J. Kakalios (unpublished).
[25] K. M. Hill and J. Kakalios (unpublished).
[26] K. Yamane *et al.* (unpublished).
[27] J. Rajchenbach, Phys. Rev. Lett. **65**, 2221 (1990).
[28] H. Henein, J. K. Brimacombe, and A. P. Watkinson, Metall. Trans. B **14B**, 207 (1983).